International Journal of Greenhouse Gas Control 4 (2010) 575–582

Contents lists available at ScienceDirect

International Journal of Greenhouse Gas Control

journal homepage: www.elsevier.com/locate/ijggc

Limitations for brine acidification due to SO_2 co-injection in geologic carbon sequestration

Brian R. Ellis, Lauren E. Crandell, Catherine A. Peters *

Department of Civil & Environmental Engineering, Princeton University, Princeton, NJ 08540, USA

ARTICLE INFO

Article history:
Received 16 March 2009
Received in revised form 20 November 2009
Accepted 23 November 2009
Available online 21 December 2009

Keywords:
SO_2
Impurities
Co-injectant
Geologic carbon storage
Acidification
Diffusion

ABSTRACT

Co-injection of sulfur dioxide during geologic carbon sequestration can cause enhanced brine acidification. The magnitude and timescale of this acidification will depend, in part, on the reactions that control acid production and on the extent and rate of SO_2 dissolution from the injected CO_2 phase. Here, brine pH changes were predicted for three possible SO_2 reactions: hydrolysis, oxidation, or disproportionation. Also, three different model scenarios were considered, including models that account for diffusion-limited release of SO_2 from the CO_2 phase. In order to predict the most extreme acidification potential, mineral buffering reactions were not modeled. Predictions were compared to the case of CO_2 alone which would cause a brine pH of 4.6 under typical pressure, temperature, and alkalinity conditions in an injection formation. In the unrealistic model scenario of SO_2 phase equilibrium between the CO_2 and brine phases, co-injection of 1% SO_2 is predicted to lead to a pH close to 1 with SO_2 oxidation or disproportionation, and close to 2 with SO_2 hydrolysis. For a scenario in which SO_2 dissolution is diffusion-limited and SO_2 is uniformly distributed in a slowly advecting brine phase, SO_2 oxidation would lead to pH values near 2.5 but not until almost 400 years after injection. In this scenario, SO_2 hydrolysis would lead to pH values only slightly less than those due to CO_2 alone. When SO_2 transport is limited by diffusion in both phases, enhanced brine acidification occurs in a zone extending only 5 m proximal to the CO_2 plume, and the effect is even less if the only possible reaction is SO_2 hydrolysis. In conclusion, the extent to which co-injected SO_2 can impact brine acidity is limited by diffusion-limited dissolution from the CO_2 phase, and may also be limited by the availability of oxidants to produce sulfuric acid.

1. Introduction

Geologic sequestration of carbon dioxide has come to the forefront of potential carbon mitigation strategies (IPCC, 2005). Sequestration in deep saline formations is an especially attractive option due to the availability of injection sites, large potential storage capacity and technical feasibility of underground injection (Bruant et al., 2002; Bachu, 2008; Benson and Cole, 2008). One of the current challenges facing implementation of large-scale CO_2 injection projects is forming regulations or guidelines that specify the required purity of the injection stream (Pollak and Wilson, 2009). In a recent editorial, John Gale pointed out the need for sound policy concerning injection stream composition and a need for further research to better understand how co-injectants will impact the success of carbon capture and storage in geologic media (Gale, 2009).

This work focuses on co-injection of sulfur dioxide, an important environmental pollutant emitted from electric power plants, which will be a primary source of CO_2 for geologic carbon sequestration. The amount of SO_2 emitted from a plant is small relative to the amount of CO_2 emitted. Fig. 1 shows the moles SO_2 emitted annually in relation to the moles of CO_2 emitted from 382 electric power plants in the United States. In 2002, these plants accounted for 99.5% of all SO_2 power plant emissions and, collectively, released more than eight million tonnes of SO_2 to the atmosphere (Miller and Van Atten, 2004).

To regulate SO_2 emissions, the U.S. EPA uses a market-based approach through Title IV of the 1990 Clean Air Act Amendments. The total size of the SO_2 emissions allowance market in the United States is on the order of $5 billion, based on a snapshot of the market in mid 2007 (EPA, 2009). It is generally believed that the collective costs are far smaller than the net benefits of SO_2 regulation in light of protection of human health and the environment (Chestnut and Mills, 2005). However, the fact remains that the power industry deems it economically favorable to, collectively, spend billions of dollars for the right to emit SO_2 rather than to control it. With the emergence of carbon capture and

* Corresponding author. Tel.: +1 609 258 5645; fax: +1 609 258 2760.
E-mail address: cap@princeton.edu (C.A. Peters).

1750-5836/$ – see front matter © 2009 Elsevier Ltd. All rights reserved.
doi:10.1016/j.ijggc.2009.11.006

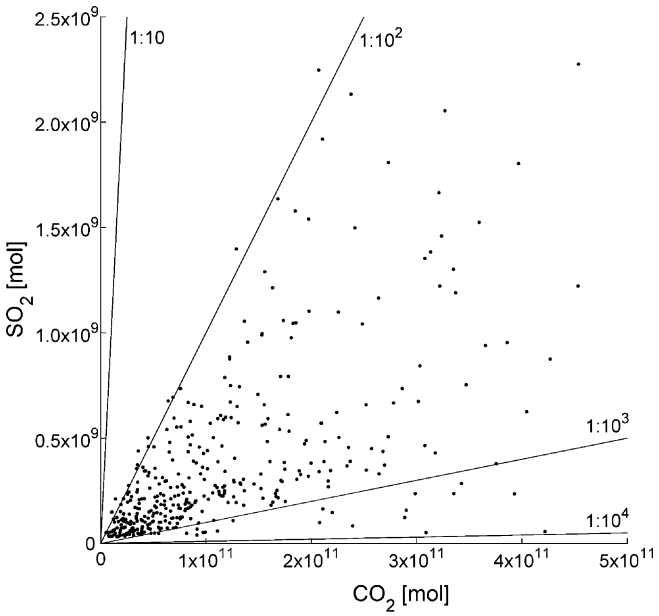

Fig. 1. Annual power plant emissions of SO_2 relative to CO_2 emissions for the highest SO_2-emitting plants in the United States (Miller and Van Atten, 2004). Lines represent ratios of molar quantities of SO_2 to CO_2.

geologic sequestration, and the possibility of SO_2 co-injection, the economic favorability of emitting SO_2 to the atmosphere could change.

A primary concern surrounding geologic carbon sequestration is the potential for brine acidification. Injection of CO_2 alone would lead to the formation of carbonic acid and cause brine acidification. This will lead to acid-catalyzed mineral dissolution and subsequent precipitation (Gunter and Perkins, 1993; Baines and Worden, 2004; Xu et al., 2004; Giammar et al., 2005; Li et al., 2006; Zerai et al., 2006; Gaus et al., 2008; Peters, 2009). Dissolution of minerals containing divalent metal cations can lead to mineral trapping of the injected carbon in the form of stable carbonate precipitates (Xu et al., 2003, 2005; Soong et al., 2004). These reactions will alter formation permeability and porosity and may be deleterious to formation integrity (Kaszuba et al., 2005). However, mineral dissolution may also lead to pH buffering as has been observed in the CO_2 injection into the Frio formation (Kharaka et al., 2006). If formation mineralogy has insufficient buffering capacity, acidified brine may degrade cements of nearby abandoned wells or alter the integrity of the caprock, thereby increasing the probability of CO_2 leakage to the surface (Gaus et al., 2005; Nordbotten et al., 2005; Carey et al., 2007; Duguid et al., 2007; Gherardi et al., 2007; Kutchko et al., 2007).

The presence of co-injectants, such as SO_2, may lead to further brine acidification through the formation of stronger acids. Both SO_2 and H_2S have been previously studied as co-injectants in the context of geologic carbon sequestration (Gunter et al., 2000; Knauss et al., 2005; Palandri and Kharaka, 2005; Xu et al., 2007). Knauss et al. (2005) predicted that co-injection of even a small amount of SO_2 (10^{-6} bar partial pressure) would lead to a brine pH of unity and enhanced mineral dissolution. This extreme acidification was attributed to the formation of sulfuric acid. Supporting evidence for extreme brine acidification due to co-injection of SO_2 was predicted by Xu et al. (2007) whose reactive transport simulations demonstrated that SO_2 co-injection into a quartzose lithic arkose formation would lead to near-zero pH values within a radial distance exceeding 100 m from the point of injection.

Although previous studies have demonstrated that co-injection of SO_2 is likely to cause enhanced brine acidification, the rate of dissolution of the injected SO_2 has never been assumed to be a limiting factor for brine acidification. Injected SO_2 will exist within a separate supercritical CO_2 ($scCO_2$) phase in the formation. As SO_2 is much more soluble in water than CO_2, it has the potential to extensively partition into the brine phase. This explains how small amounts of SO_2 can cause significant brine acidification as previously predicted (Knauss et al., 2005; Xu et al., 2007). However, the work of Crandell et al. (in press) has shown that mass transfer limitations of SO_2 through the $scCO_2$ phase may be important. That work demonstrated that SO_2 within the $scCO_2$ plume near the phase boundary is quickly depleted. This establishes a thick zone of depletion which creates resistance to further SO_2 mass transfer, resulting in less than a third of the injected SO_2 dissolving into the brine phase after 1000 years.

The goal of this modeling effort is to gain a more thorough understanding of the magnitude and time scale of brine acidification for the case of SO_2 co-injection during geologic carbon sequestration in deep saline formations. The potential for brine acidification is investigated for three different SO_2 reaction scenarios: hydrolysis, oxidation, and disproportionation, to investigate the effects of different sulfur-bearing acids. The model scenarios that are studied describe the situation in which SO_2 mass transport to the brine phase is limited by diffusion in the $scCO_2$ phase. One model describes rapid dispersion of SO_2 in a slowly advecting brine phase. The other model investigates diffusive transport of SO_2 in a stagnant brine phase. These represent extreme end cases for transport limitations and are meant to provide bounding estimates of brine acidification, as in reality, a combination of advective and diffusive transport in the aqueous phase will exist. For comparison, we model the case of SO_2 phase equilibrium between the entire volumes of $scCO_2$ and brine, which represents the maximum potential basin-scale acidification. To predict brine pH, we developed a geochemical model that simulates aqueous speciation and thermodynamic phase equilibrium of injected CO_2 and SO_2 with brine from a Mississippian carbonate formation in the Alberta Basin, Canada.

2. Methods

2.1. SO_2 reaction scenarios

Three different scenarios for reaction in the brine phase were investigated. The first is that of SO_2 hydrolysis,

$$SO_2 + H_2O \Leftrightarrow H_2SO_3$$

This reaction produces only the weak acid, sulfurous acid. If this is the only reaction occurring, it represents the case of there being no mechanism for oxidation of SO_2. When oxidizing conditions exist, SO_2 is oxidized following the reaction:

$$SO_2 + H_2O + \tfrac{1}{2}O_2 \Leftrightarrow H_2SO_4$$

This produces sulfuric acid, a very strong acid. While this reaction is written with molecular oxygen as the oxidant, a typical oxygen fugacity in deep saline formations is on the order of 10^{-63} bar (Helgeson et al., 1993). It is unlikely that this is sufficient to drive the SO_2 oxidation reaction to completion, so here, molecular oxygen as a reactant is intended to be representative of all potential oxidants. Strong oxidants, such as MnO, are likely to exist in sufficient quantities to oxidize the small amount of injected SO_2. This assumption is in line with the work of Knauss et al. (2005).

The third scenario that is modeled is SO_2 disproportionation,

$$SO_2 + H_2O \Leftrightarrow \tfrac{3}{4}H_2SO_4 + \tfrac{1}{4}H_2S$$

In this reaction scenario, the sulfur in SO_2 is both oxidized to sulfate and reduced to sulfide in a ratio of 3:1. In the context of SO_2 co-injection during geologic carbon sequestration, disproportionation has been previously modeled as the dominant mechanism of acid formation (Palandri and Kharaka, 2005; Xu et al., 2007). This reaction is typically associated with hydrothermal systems. Holland (1965) demonstrated through thermochemical modeling that nearly all SO_2 of magmatic origin is consumed via disproportionation. As magmatic gases are cooled, SO_2 reacts with condensed water vapor to form sulfuric acid and the weaker acid, hydrogen sulfide (Holland, 1965; Rye et al., 1992; Kusakabe et al., 2000; Symonds et al., 2001).

2.2. Model system and conditions

To estimate the impact of SO_2 on brine chemistry, a two-phase system was modeled consisting of a $scCO_2$ phase containing a small amount of SO_2 and a brine phase. Consistent with the simplified geometry used by Crandell et al. (in press), the injected gas phase was modeled as a cone-shaped plume (Fig. 2). The cone radius of 2.8 km corresponds to a formation with 20% porosity and a thickness of 75 m. Together with the brine phase under the cone, the system is a cylinder of diameter equal to that of the $scCO_2$ cone and height corresponding to the formation thickness. The injection formation is assumed to be bounded on the top and bottom by impermeable formations. Model simplifications, including the absence of CO_2 flow and the absence of residual brine, are discussed along with the implications in Crandell et al. (in press).

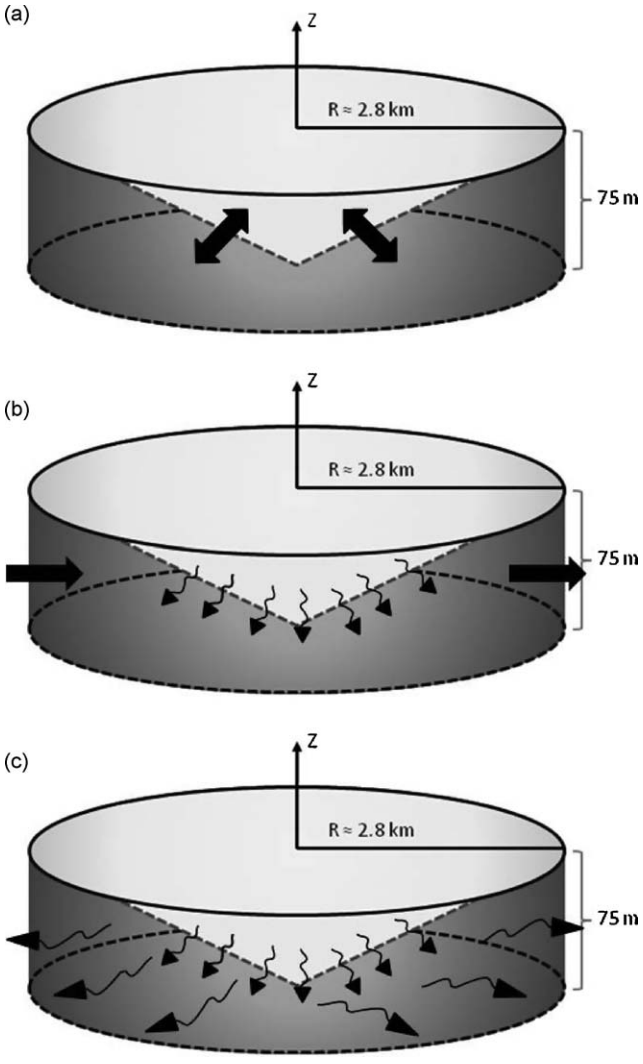

Fig. 2. Schematic diagram of model system showing the $scCO_2$ plume (light gray) and brine volume (dark gray): (a) SO_2 phase equilibrium between the CO_2 and brine phases; (b) diffusion-limited SO_2 dissolution with uniform sulfur distribution in an advecting brine phase; (c) diffusion-limited SO_2 dissolution with diffusive transport of SO_2 in a stagnant brine phase.

Table 1
Brine composition.

Species	[mol/L]	[mg/L]
Na^+	8.65×10^{-1}	19,900
Cl^-	8.61×10^{-1}	30,500
Ca^{2+}	9.98×10^{-3}	400
Mg^{2+}	6.99×10^{-3}	170
SO_4^{2-}	3.44×10^{-4}	33
HCO_3^-	3.75×10^{-2}	2290
pH	7.8	

Source: Michael (2002).

System conditions were 40 °C and 127 bar, which correspond to an injection depth of 1.2 km assuming a pressure gradient of 105 bar/km, a thermal gradient of 25 °C/km (Van der Meer, 1993; Bachu, 2000), and a surface temperature of 10 °C. Under these conditions, CO_2 will exist as a supercritical fluid. The total volume of the injected CO_2–SO_2 mixture was 1.2×10^8 m^3. This was determined based upon a 50-year injection period at a rate of 1.83 Mtonne/year (Wilson and Monea, 2004) and a mixture density of 774 kg/m^3 (Crandell et al., in press).

The mixture composition was chosen to be 99% CO_2 and 1% SO_2, as this is within the range of relative CO_2 to SO_2 emissions shown in Fig. 1. Initial conditions for both diffusive models were such that SO_2 was assumed to be uniformly distributed throughout the $scCO_2$ plume. The initial brine composition used in all modeling is shown in Table 1; it is taken from an analysis of a Mississippian carbonate aquifer from the Alberta sedimentary basin, Canada (Michael, 2002). The analysis is an uncorrected well-head formation fluid measurement.

The phase equilibrium and diffusive transport models developed for this work are coupled with a geochemical model describing instantaneous reaction and speciation in the aqueous phase. All model codes were written in Matlab® (Version 7.6.0.324 R2008a, The MathWorks™).

2.3. Geochemical model

In the geochemical model, an iterative process was used to compute aqueous speciation of carbonates, sulfates, sulfites and hydrogen sulfide. As needed, aqueous speciation was coupled with phase equilibrium of SO_2 and CO_2. The SO_2 reactions were examined individually, such that in a given simulation only one of the three possible reaction scenarios was modeled. For the case of SO_2 oxidation, oxygen fugacity was held constant at 10^{-2} bar to represent full oxidation of the injected SO_2. The brine pH was determined by convergence on a solution for conservation of mass and balance of charge.

All aqueous speciation reactions are assumed to be instantaneous and are shown with their equilibrium constants in Table 2. Reaction equilibrium constants were adjusted for high temperature and pressure conditions using SUPCRT92 (Johnson et al., 1992). Also shown in Table 2 are the equilibrium constants for aqueous solubility of SO_2 and CO_2. For SO_2, the value shown is the pressure- and temperature-adjusted Henry's Law constant estimated by Crandell et al. (in press) for a 1 M NaCl solution at 40 °C and 127 bar. The SO_2 fugacity coefficient in the $scCO_2$ was determined following the method of Tarakad and Danner (1977). The semi-empirical model of Duan and Sun (2003) was used to calculate CO_2 solubility. Aqueous species activity

Table 2
Reactions considered in the geochemical model.

Reaction	$\log(K_{eq})$	$\log(K_H$ [mol L^{-1} bar^{-1}])
$SO_{2(aq)} + H_2O \Leftrightarrow H_2SO_3$	−0.042	
$SO_3^{2-} + \frac{1}{2}O_{2(g)} \Leftrightarrow SO_4^{2-}$	42.86	
$SO_{2(aq)} + H_2O \Leftrightarrow \frac{3}{4}HSO_4^- + \frac{3}{4}H^+ + \frac{1}{4}H_2S_{(aq)}$	5.68	
$H_2CO_3^* \Leftrightarrow HCO_3^- + H^+$	−6.27	
$HCO_3^- \Leftrightarrow CO_3^{2-} + H^+$	−10.16	
$H_2SO_3 \Leftrightarrow HSO_3^- + H^+$	−1.93	
$HSO_3^- \Leftrightarrow SO_3^{2-} + H^+$	−7.24	
$HSO_4^- \Leftrightarrow SO_4^{2-} + H^+$	−2.12	
$H_2O \Leftrightarrow OH^- + H^+$	−13.49	
$SO_{2(scCO_2)} \Leftrightarrow SO_{2(aq)}$		−0.23[a]
$CO_{2(scCO_2)} + H_2O \Leftrightarrow H_2CO_3^*$		−1.99

[a] From Crandell et al. (in press).

Table 3
Diffusion coefficients.

Species	Diffusion coefficient [m^2/s]
$SO_{2(scCO_2)}$[a]	2.49×10^{-08}
$SO_{2(aq)}$	2.31×10^{-09}
H_2SO_3	2.31×10^{-09}
HSO_3^-	1.62×10^{-09}
SO_3^{2-}	1.01×10^{-09}
HSO_4^-	1.45×10^{-09}
SO_4^{2-}	1.12×10^{-09}
$CO_{2(aq)}$	2.73×10^{-09}
HCO_3^-	1.24×10^{-09}
CO_3^{2-}	9.68×10^{-10}

[a] From Crandell et al. (in press).

coefficients were calculated via the extended Debye–Huckel formalism of Helgeson and Kirkham (1974).

In order to predict the most extreme acidification potential, mineral buffering reactions were not included in any of the simulations performed in this study. For further simplicity, aqueous complexation reactions were also not included.

2.4. Phase equilibrium model

In the phase equilibrium model scenario, all the brine is assumed to be in equilibrium with the SO_2 and CO_2 in the entire $scCO_2$ phase (Fig. 2(a)). According to the system geometry, the ratio of the volumes of brine to $scCO_2$ phases is 2:1. Initial brine alkalinity was varied to test the sensitivity of equilibrium pH to initial brine composition under each of the three reaction scenarios. Brine alkalinity was modeled as bicarbonate and ranged from 1×10^{-3} M to 1 M.

2.5. Diffusion modeling

The first diffusion model considers SO_2 diffusion limitations in the $scCO_2$ phase and uniform sulfur distribution in a slowly advecting brine phase (Fig. 2(b)). This model is meant to simulate rapid dispersion in the aqueous phase. Fresh brine is introduced at each time step to simulate advective flow within the brine portion of the model system. Flow rates of 1 m/year and 0.1 m/year were modeled by computing a residence time using the diameter of the cylindrical model system as the length scale for advective flow. At each time step SO_2 and CO_2 are allowed to reach saturation at the brine phase boundary and are then uniformly distributed throughout the brine phase. This model assumes a constant total system volume allowing for increasing brine volume as the $scCO_2$ phase is depleted.

The second diffusion model considers diffusion in both phases (Fig. 2(c)) and is meant to simulate the case of a stagnant brine phase. In the brine phase at a distance of 1 km beyond the radial extent of the $scCO_2$ plume, a constant concentration boundary condition was set to be equal to the background sulfate and bicarbonate concentrations shown in Table 1. SO_2 and CO_2 concentrations in the brine phase at the plume boundary were determined by solubility limitations. For CO_2, this effectively represents a constant concentration boundary condition for the brine-side of the system.

In both cases, the diffusion modeling builds upon the modeling presented in Crandell et al. (in press) by including brine phase transport and geochemical reactions. All diffusion modeling uses a time step of 0.25 years. See Crandell et al. (in press) for further detail regarding model equations and the numerical discretization scheme. Previously, SO_2 flux to the brine phase was calculated assuming no build-up of sulfur in the brine phase (Crandell et al., in press); however, in this study SO_2 concentration in the brine is governed by both solubility constraints and the thermodynamics of each SO_2 reaction scenario. Diffusive flux of SO_2 into the brine phase was determined by simultaneously solving for phase partitioning and thermodynamic equilibrium of the aqueous geochemical reactions via an iterative process at each boundary cell. No flux boundaries are imposed at the top and bottom of the injection formation in both diffusive models, corresponding to the injection formation being bounded by impermeable caprocks.

The diffusion coefficient for SO_2 within the $scCO_2$ phase was taken from Crandell et al. (in press). For the second diffusion model, aqueous diffusion coefficients for neutral species were determined via the Wilke–Chang equation (Wilke and Chang, 1955) using an updated association parameter for water from Hayduk and Laudie (1974). Aqueous diffusion coefficients for ionic species were determined via the Nernst–Haskell equation (Robinson and Stokes, 1965; Vanysek, 2009). Diffusion coefficients are given in Table 3.

3. Results

The brine pH results from the phase equilibrium model scenario are shown in Fig. 3 for an initial brine alkalinity of 3.75×10^{-2} M. For all three SO_2 reaction scenarios, mass balance modeling showed that equilibrium partitioning would cause more than 99.8% of the SO_2 to partition into the brine phase. All three scenarios are predicted to produce significant acidification beyond a pH of 4.6 that would result from dissolution of pure CO_2. SO_2 oxidation is predicted to cause the most severe brine acidification with a pH of 1.1. SO_2 disproportionation causes a similar degree of acidification. While SO_2 hydrolysis produces a weaker acid, it would still significantly reduce the pH.

Fig. 4 shows how variation in initial brine alkalinity is predicted to impact equilibrium pH. In the case of pure CO_2, the brine pH varies gradually from 3.2 for 10^{-3} M alkalinity to 6.1 for 1 M. For each of the three SO_2 reaction scenarios, an inflection in the brine pH curve is predicted indicating the alkalinity at which the acidity would be titrated. The absence of a distinct titration point for the case of pure CO_2 is due to the fact that it remains in excess, whereas only a limited amount of acid is generated from the dissolved SO_2. For the case of SO_2 hydrolysis, titration occurs at a lower alkalinity than for the other two reactions because hydrolysis is less thermodynamically favorable and produces less acid.

Brine pH results from the diffusion model investigating rapid brine phase dispersion are displayed in Fig. 5, for two brine flow rates. The results from SO_2 disproportionation are very similar to those for oxidation, so only results for SO_2 oxidation and SO_2 hydrolysis are shown. For reference, brine pH evolution for the case of a pure CO_2 injection plume is also shown. The system brine reaches CO_2 saturation after 150 years, for a flow rate of 1 m/year. As CO_2 dissolves, the $scCO_2$-brine boundary moves inward a few meters, corresponding to a 12% reduction in the total $scCO_2$ volume after 1000 years.

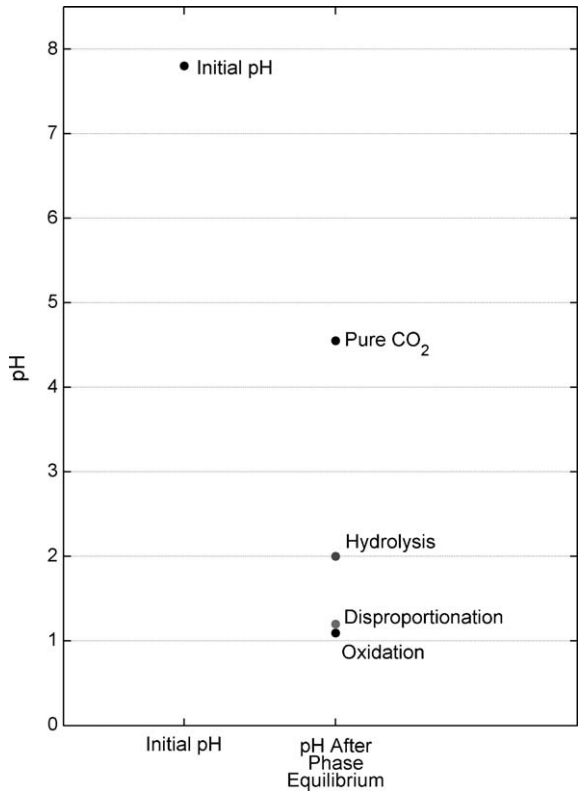

Fig. 3. Phase equilibrium brine pH results for each of the three reactions and CO_2 alone for an initial alkalinity of 3.75×10^{-2} M.

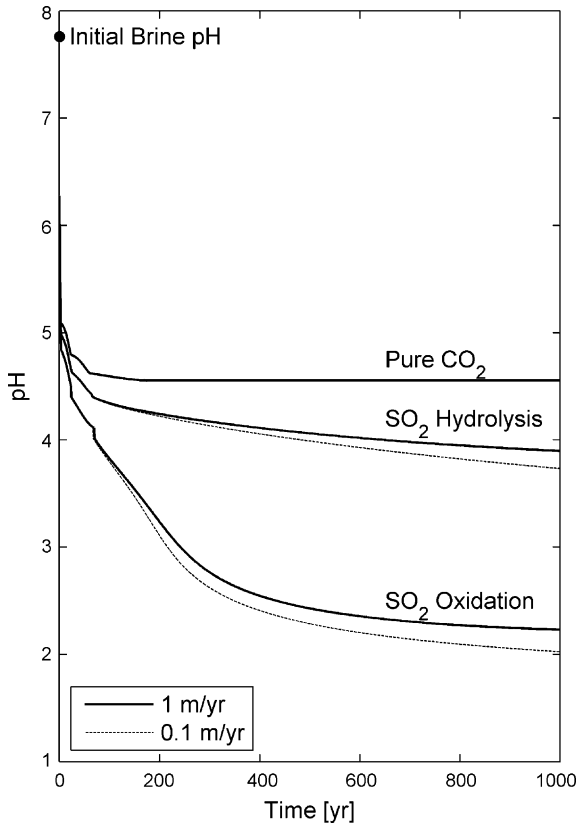

Fig. 5. Brine pH results for SO_2 hydrolysis and SO_2 oxidation reaction scenarios for diffusion-limited SO_2 dissolution into an advecting brine. For reference, pH results for the case of a pure CO_2 injection plume are also shown.

The case of SO_2 oxidation is again predicted to cause the most severe brine acidification, but hundreds of years would need to pass before this is manifested. Enhanced brine acidification beyond a pH of 4.6, caused by CO_2 alone, is not predicted to occur until after 25 years for the case of SO_2 oxidation. Brine pH values below 3 are not predicted to occur until after nearly 200 years when SO_2 is oxidized to sulfuric acid. At 200 years, only 20% of the total injected sulfur is predicted to have dissolved. At the end of the 1000-year simulation, brine pH values near 2 and 4 are predicted for the cases of SO_2 oxidation and hydrolysis, respectively. Slightly higher pH values are predicted for a higher brine flow rate due to the increased rate of flushing from the system. After 1000 years, just over 35% of the injected sulfur is predicted to have dissolved.

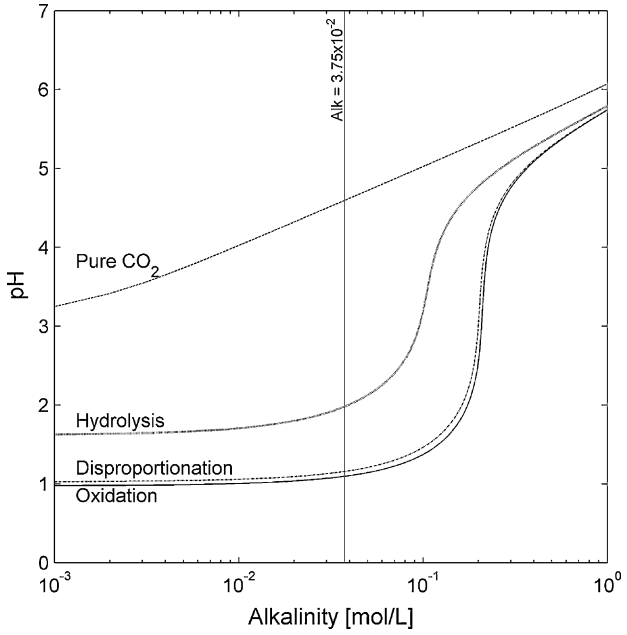

Fig. 4. Phase equilibrium brine pH results for a range of values of initial brine alkalinity, for CO_2 alone and each of the three reaction scenarios.

Diffusion modeling results for the case of a stagnant brine phase are shown in Figs. 6 and 7. The results are presented at snapshots in time as a cross-section drawn from the center of the $scCO_2$ plume to 200 m beyond the radial extent of the plume. The figures show pH contours within the brine phase and SO_2 concentration contours within the $scCO_2$ phase. As the results for SO_2 oxidation and disproportionation are again very similar, only results for SO_2 oxidation and hydrolysis are presented. Fig. 6 shows simulation results for SO_2 hydrolysis after 500 and 1000 years. Here, pH values near 2 are predicted to occur adjacent to the plume boundary; however, enhanced brine acidification beyond that caused by CO_2 alone (pH = 4.6) is not predicted to occur beyond 4 m of the plume boundary. Build-up of dissolved SO_2 at the plume boundary causes a significant reduction in the flux of SO_2 from the $scCO_2$ phase, resulting in less than 10% of the injected sulfur dissolving after 1000 years.

Fig. 7 shows the results for the case of SO_2 oxidation. Brine pH values near zero are predicted proximal to the $scCO_2$-brine phase boundary, but enhanced acidification beyond a pH of 4.6 is not predicted to occur beyond 5 m of the plume boundary. In this simulation, dissolved SO_2 does not substantially build-up adjacent to the plume boundary as SO_2 is readily oxidized to sulfuric acid. In fact, the SO_2 concentration profile is effectively identical to the case of a zero concentration of SO_2 adjacent to the plume boundary simulated by Crandell et al. (in press). Compared to SO_2 hydrolysis,

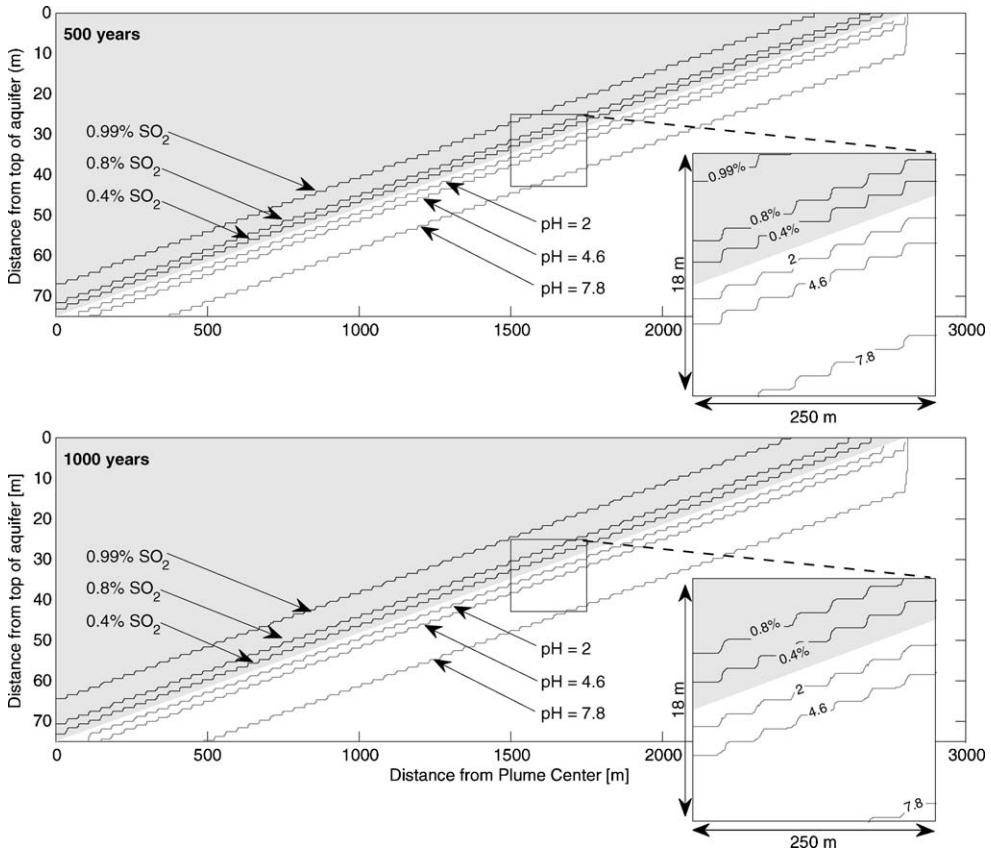

Fig. 6. Cross-section showing results from diffusion-limited SO_2 mass transport in both the $scCO_2$ and brine phases. For the case of SO_2 hydrolysis, contours show SO_2 concentration in the $scCO_2$ phase and pH in the brine phase after 500 and 1000 years. Shaded region denotes $scCO_2$ phase.

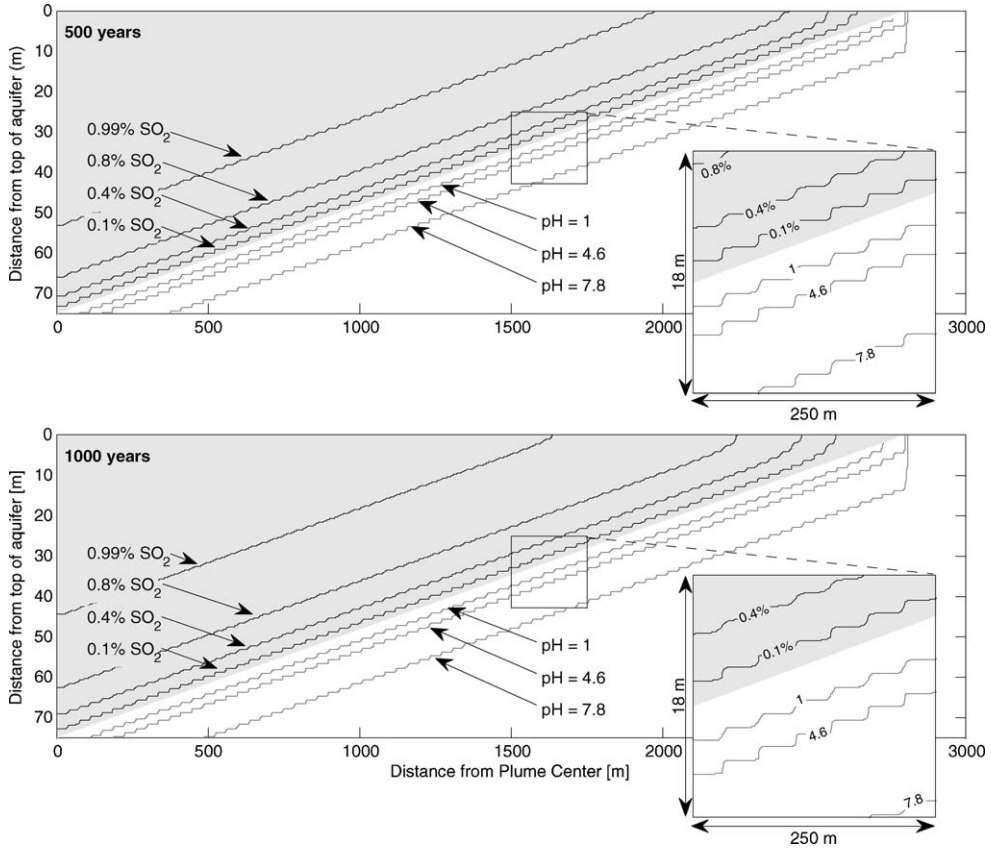

Fig. 7. Cross-section showing results from diffusion-limited SO_2 mass transport in both the $scCO_2$ and brine phases. For the case of SO_2 oxidation, contours show SO_2 concentration in the $scCO_2$ phase and pH in the brine phase after 500 and 1000 years. Shaded region denotes $scCO_2$ phase.

the case of oxidation results in a greater flux of SO_2 from the $scCO_2$ phase leading to approximately 27% of the injected SO_2 dissolving after 1000 years.

4. Discussion

The results from this study confirm that SO_2 co-injection will lead to increased brine acidification relative to the case of injection of pure CO_2, but the magnitude depends on the rate of SO_2 dissolution, redox conditions in the formation, hydrodynamic conditions controlling the zone of influence, and buffering potential of the formation. For the scenario of instantaneous and complete phase equilibrium across the entire system, extensive partitioning of SO_2 to the brine phase and significant brine acidification is predicted. However, this scenario is unrealistic due to the absence of fast fluid flows that would produce rapid mixing and extensive contact between the two phases. It is more likely that SO_2 mass transfer to the formation brine will be limited by slow diffusion through the $scCO_2$ phase (Crandell et al., in press). Our modeling results show that when this is the case, SO_2 co-injection will not lead to brine acidification as severe as has been previously predicted (Knauss et al., 2005; Xu et al., 2007). Diffusion limitations will slow the rate at which SO_2 will dissolve into the brine. To a large extent, SO_2 is predicted to remain in the $scCO_2$ plume even after 1000 years. This means that acidification will persist for a long time, but the magnitude of this acidification is not nearly as severe as that predicted when SO_2 mass transport to the brine is not a limiting factor.

All three SO_2 reaction scenarios predicted enhanced brine acidification, but consistently, SO_2 oxidation caused the most severe acidification. This is not surprising given that, for this reaction, the SO_2 is oxidized to the very strong acid, sulfuric acid. This will occur only if oxidizing conditions exist in the injection formation. If SO_2 is not oxidized, only the weak acid, sulfurous acid, is produced via SO_2 hydrolysis. This acid will cause less severe acidification and is more easily titrated by brine alkalinity. SO_2 hydrolysis alone would create the minimum potential for brine acidification, and SO_2 oxidation would create the maximum potential. In this work, these have been modeled in isolation but in reality it is likely that the fate of dissolved SO_2 will be determined by a combination of the different possible SO_2 reaction scenarios.

If SO_2 disproportionation occurs, it will lead to a similar degree of brine acidification to that of full SO_2 oxidation, providing supporting evidence to the work of Xu et al. (2007) who established that disproportionation of co-injected SO_2 will lead to significant brine acidification. As SO_2 disproportionation occurs via simultaneous oxidation and reduction of the sulfur in SO_2, the favorability of this reaction is not dependent on the availability of other oxidants. This implies that this reaction has the potential to occur regardless of the local redox conditions and if it occurs, it will likely occur coincidentally with either SO_2 hydrolysis or oxidation.

The models in this study present pH estimates for bounding aqueous transport-limiting scenarios, however, in reality SO_2 will be dispersed via a combination of advective and diffusive transport. Regardless of aqueous transport conditions, slow diffusion in the $scCO_2$ will reduce the potential for brine acidification due to SO_2 co-injection. Slow diffusion of SO_2 in the $scCO_2$ prevents basin-wide brine acidification from occurring for several centuries. In this same timeframe, pH-buffering mineral dissolution reactions are likely to occur. These reactions have the potential to buffer much of the acid generated by SO_2 dissolution as long as the recipient formation has sufficient carbonate, basic silicate or basic aluminosilicate minerals (Gunter et al., 2000).

It is most likely that potential injection formations will have very slow-moving brines and diffusion will play a major role in determining aqueous phase transport. This would suggest that acidification of the injection formation brine will occur over a similar spatial and temporal scale as that predicted for the case of a stagnant brine phase. Here, even after 1000 years, brine acidification below a pH of 4.6 is not predicted to occur beyond 5 m of the injection plume boundary. This is a much smaller zone of extreme acidification than the roughly 100 m zone predicted by Xu et al. (2007) for a 1D system which allowed for both advection and diffusion in the brine. As demonstrated by Xu et al. (2007), severe mineral dissolution within this highly acidified zone may be likely. Enhanced mineral dissolution due to SO_2 co-injection may eventually lead to enhanced mineral trapping of injected CO_2 in the form of secondary carbonate mineral precipitates (Knauss et al., 2005; Palandri and Kharaka, 2005; Xu et al., 2007).

5. Summary and conclusions

This study has demonstrated that SO_2 co-injection during geologic carbon sequestration has the potential to cause enhanced brine acidification, but that the magnitude, onset, and spatial extent of this acidification may not be significant. When SO_2 mass transfer limitations are not accounted for, brine pH values near unity are predicted. However, we predict that diffusion limitations can cause 73–90% of the injected SO_2 to remain within the $scCO_2$ phase after 1000 years. Furthermore, if potential oxidants are not present, severe brine acidification will occur only if SO_2 disproportionation is favorable. Even for the case of rapid aqueous phase dispersion, pH values below 3 are not reached for several hundred years. As mineral dissolution and resultant pH buffering is likely to occur during this same timeframe, the potential for brine acidification would be further reduced.

In conclusion, the co-injection of a small amount of SO_2 is not predicted to cause rapid, severe widespread brine acidification. This suggests that co-injection may be a viable option for mitigating SO_2 emissions from power plants and should be considered in future policy regarding injection stream purity.

Our results highlight the potential disparity in estimating brine pH if dissolution limitations are not accounted for. As brine pH will impact water–rock interactions, the manner in which SO_2 dissolution is modeled is an important consideration in any geochemical modeling effort investigating SO_2 co-injection.

Acknowledgements

Financial support for this project came from the Department of Energy, Office of Basic Energy Sciences, through Grant No. DE-FG02-05ER15636. Dr. Stephan Bachu, Dr. Maja Buschkuehle, and Dr. Karsten Michael, formerly of the Alberta Geological Survey, were helpful in providing access to brine chemistry data used in this study. We would also like to thank two anonymous reviewers for their constructive suggestions for improving the quality of the manuscript.

References

Bachu, S., 2000. Sequestration of CO_2 in geological media: criteria and approach for site selection in response to climate change. Energ. Convers. Manage. 41 (9), 953–970.

Bachu, S., 2008. CO_2 storage in geological media: role, means, status and barriers to deployment. Prog. Energ. Combust. 34 (2), 254–273.

Baines, S.J., Worden, R.H., 2004. The long-term fate of CO_2 in the subsurface: natural analogues for CO2 storage. In: Baines, S.J., Worden, R.H. (Eds.), Geological Storage of Carbon Dioxide, vol. 233. Geological Society, London, Special Publications, pp. 59–85.

Benson, S.M., Cole, D.R., 2008. CO_2 sequestration in deep sedimentary formations. Elements 4 (5), 325–331.

Bruant, R.G., Guswa, A.J., Celia, M.A., Peters, C.A., 2002. Safe storage of CO_2 in deep saline aquifers. Environ. Sci. Technol. 26 (11), 240a–245a.
Carey, J.W., Wigand, M., Chipera, S.J., WoldeGabriel, G., Pawar, R., Lichtner, P.C., Wehner, S.C., Raines, M.A., Guthrie, G.D., 2007. Analysis and performance of oil well cement with 30 years of CO_2 exposure from the SACROC Unit, West Texas, USA. Int. J. Greenhouse Gas Control 1 (1), 75–85.
Chestnut, L.G., Mills, D.M., 2005. A fresh look at the benefits and costs of the US Acid Rain Program. J. Environ. Manage. 77 (3), 252–266.
Crandell, L.E., Ellis, B.R., Peters, C.A., in press. Dissolution potential of SO_2 co-injected with CO_2 in geologic sequestration. Environ. Sci. Technol., doi:10.1021/es902612m.
Duan, Z.H., Sun, R., 2003. An improved model calculating CO_2 solubility in pure water and aqueous NaCl solutions from 273 to 533 K and from 0 to 2000 bar. Chem. Geol. 193 (3–4), 257–271.
Duguid, A., Radonjic, M., Scherer, G.W., 2007. The effect of carbonated brine on well cement used in geologic formations, paper TH4-10.2. ISBN 978-0-660-19695-4 In: Beaudoin, J.J., Makar, J.M., Raki, L. (Eds.), Proc. 12th ICCC, National Research Council of Canada, Montreal, Canada.
EPA, U.S., Acid Rain and Related Programs 2007 Progress Report, 2009. U.S. Environmental Protection Agency: Washington, DC.
Gale, J., 2009. Impure thoughts. Int. J. Greenhouse Gas Control 3 (1), 1–2.
Gaus, I., Audigane, P., Andre, L., Lions, J., Jacquemet, N., Dutst, P., Czernichowski-Lauriol, I., Azaroual, M., 2008. Geochemical and solute transport modelling for CO_2 storage, what to expect from it? Int. J. Greenhouse Gas Control 2 (4), 605–625.
Gaus, I., Azaroual, M., Czernichowski-Lauriol, I., 2005. Reactive transport modelling of the impact of CO_2 injection on the clayey cap rock at Sleipner (North Sea). Chem. Geol. 217 (3–4), 319–337.
Gherardi, F., Xu, T.F., Pruess, K., 2007. Numerical modeling of self-limiting and self-enhancing caprock alteration induced by CO_2 storage in a depleted gas reservoir. Chem. Geol. 244 (1–2), 103–129.
Giammar, D.E., Bruant Jr., R.G., Peters, C.A., 2005. Forsterite dissolution and magnesite precipitation at conditions relevant for deep saline aquifer storage and sequestration of carbon dioxide. Chem. Geol. 217, 257–276.
Gunter, W.D., Perkins, E.H., 1993. Aquifer disposal of CO_2-rich gases—reaction design for added capacity. Energ. Convers. Manage. 34, 941–948.
Gunter, W.D., Perkins, E.H., Hutcheon, I., 2000. Aquifer disposal of acid gases: modelling of water–rock reactions for trapping of acid wastes. Appl. Geochem. 15 (8), 1085–1095.
Hayduk, W., Laudie, H., 1974. Prediction of diffusion coefficients for nonelectrolytes in dilute aqueous solutions. AIChE J. 20 (3), 611–615.
Helgeson, H.C., Kirkham, D.H., 1974. Theoretical prediction of thermodynamic behavior of aqueous electrolytes at high pressures and temperatures. 2. Debye–Huckel parameters for activity-coefficients and relative partial molal properties. Am. J. Sci. 274, 1199–1261.
Helgeson, H.C., Knox, A.M., Owens, C.E., Shock, E.L., 1993. Petroleum, oil field waters, and authigenic mineral assemblages: are they in metastable equilibrium in hydrocarbon reservoirs? Geochim. Cosmochim. Ac. 57, 3295–3339.
Holland, H.G., 1965. Some applications of thermochemical data to problems of ore deposits. II. Mineral assemblages and the composition of ore-forming fluids. Econ. Geol. Bull. Soc. 60 (6), 1101–1166.
International Panel on Climate Change (IPCC), 2005. In: Metz, B., Davidson, O., de Coninck, H., Loos, M., Meyer, L. (Eds.), Special Report on Carbon Dioxide Capture and Storage. Cambridge University Press, Cambridge, U.K., pp. 195–276.
Johnson, J.W., Oelkers, E.H., Helgeson, H.C., 1992. SUPCRT92–a software package for calculating the standard molal thermodynamic properties of minerals, gases, aqueous species, and reactions from 1 to 5000 bar and 0 to 1000 °C. Comput. Geosci. 18, 899–947.
Kaszuba, J.P., Janecky, D.R., Snow, M.G., 2005. Experimental evaluation of mixed fluid reactions between supercritical carbon dioxide and NaCl brine: relevance to the integrity of a geologic carbon repository. Chem. Geol. 217, 277–293.
Kharaka, Y.K., Cole, D.R., Hovorka, S.D., Gunter, W.D., Knauss, K.G., Freifeld, B.M., 2006. Gas–water–rock interactions in Frio Formation following CO_2 injection: implications for the storage of greenhouse gases in sedimentary basins. Geology 34, 577–580.
Knauss, K.G., Johnson, J.W., Steefel, C.I., 2005. Evaluation of the impact of CO_2, co-contaminant gas, aqueous fluid and reservoir rock interactions on the geologic sequestration of CO_2. Chem. Geol. 217 (3–4), 339–350.
Kusakabe, M., Komoda, Y., Takano, B., Abiko, T., 2000. Sulfur isotopic effects in the disproportionation reaction of sulfur dioxide in hydrothermal fluids: implications for the delta S-34 variations of dissolved bisulfate and elemental sulfur from active crater lakes. J. Volcanol. Geoth. Res. 97, 287–307.
Kutchko, B.G., Strazisar, B.R., Dzombak, D.A., Lowry, G.V., Thaulow, N., 2007. Degradation of well cement by CO_2 under geologic sequestration conditions. Environ. Sci. Technol. 41 (13), 4787–4792.
Li, L., Peters, C.A., Celia, M.A., 2006. Upscaling geochemical reaction rates using pore-scale network modeling. Adv. Water Resour. 29, 1351–1370.
Michael, K., 2002. Flow of formation water in the Alberta Basin adjacent to the Rocky Mountains thrust and fold belt, west-central Alberta, Canada. Ph.D. Dissertation. University of Alberta, Edmonton, Alberta, Canada.
Miller, P.J., Van Atten, C., 2004. North American Power Plant Air Emissions. Commission for Environmental Cooperation of North America.
Nordbotten, J.M., Celia, M.A., Bachu, S., Dahle, H.K., 2005. Semianalytical solution for CO_2 leakage through an abandoned well. Environ. Sci. Technol. 39, 602–611.
Palandri, J.L., Kharaka, Y.K., 2005. Ferric iron-bearing sediments as a mineral trap for CO_2 sequestration: iron reduction using sulfur-bearing waste gas. Chem. Geol. 217, 351–364.
Peters, C.A., 2009. Accessibilities of reactive minerals in consolidated sedimentary rock: an imaging study of three sandstones. Chem. Geol. 265 (1–2), 198–208.
Pollak, M.F., Wilson, E.J., 2009. Regulating geologic sequestration in the United States: early rules take divergent approaches. Environ. Sci. Technol. 43 (9), 3035–3041.
Robinson, R.A., Stokes, R.H., 1965. Electrolyte Solutions, 2nd edn. Butterworths, London.
Rye, R.O., Bethke, P.M., Wasserman, M.D., 1992. The stable isotope geochemistry of acid sulfate alteration. Econ. Geol. Bull. Soc. 87 (2), 225–262.
Soong, Y., Goodman, A.L., McCarthy-Jones, J.R., Baltrus, J.P., 2004. Experimental and simulation studies on mineral trapping of CO_2 with brine. Energ. Convers. Manage. 45, 1845–1859.
Symonds, R.B., Gerlach, T.M., Reed, M.H., 2001. Magmatic gas scrubbing: implications for volcano monitoring. J. Volcanol. Geoth. Res. 108, 303–341.
Tarakad, R.R., Danner, R.P., 1977. Improved corresponding states method for polar fluids—correlation of 2nd viral-coefficients. AIChE J. 23 (5), 685–695.
Van der Meer, L.G.H., 1993. The conditions limiting CO_2 storage in aquifers. Energ. Convers. Manage. 34 (9–11), 959–966.
Vanysek, P., 2009. Ionic conductivity and diffusion at infinite dilution. In: Lide, D.R. (Ed.), CRC Handbook of Chemistry and Physics. 89th edition. CRC Press/Taylor and Francis, Boca Raton, FL, pp. 5.76–5.78.
Wilke, C.R., Chang, P., 1955. Correlation of diffusion coefficients in dilute solutions. AIChE J. 1 (2), 264–270.
Wilson, M., Monea, M., 2004. IEA GHG Weyburn monitoring and storage project, summary report. In: Proceedings of the 7th International Conference on Greenhouse Gas Control Technologies, vol. III, Petroleum Technology Research Center, Regina, SK, Canada, p. 273.
Xu, T., Apps, J.A., Pruess, K., 2003. Reactive geochemical transport simulation to study mineral trapping for CO_2 disposal in deep arenaceous formations. J. Geophys. Res. -Sol. Ea. 108, 2071–2083.
Xu, T., Apps, J., Pruess, K., 2004. Numerical simulation of CO_2 disposal by mineral trapping in deep aquifers. Appl. Geochem. 19, 917–936.
Xu, T., Apps, J.A., Pruess, K., 2005. Mineral sequestration of carbon dioxide in a sandstone–shale system. Chem. Geol. 217, 295–318.
Xu, T., Apps, J.A., Pruess, K., Yamamoto, H., 2007. Numerical modeling of injection and mineral trapping of CO_2 with H_2S and SO_2 in a sandstone formation. Chem. Geol. 242 (3–4), 319–346.
Zerai, B., Saylor, B., Matisoff, G., 2006. Computer simulation of CO_2 trapped through mineral precipitation in the Rose Run Sandstone, Ohio. Appl. Geochem. 21, 223–240.